

## **THERAPEUTIC IMPLICATIONS OF BONE MARROW MESENCHYMAL STEM CELLS IN EXPERIMENTAL LIVER FIBROSIS**

**Hanaa H. Ahmed<sup>1\*</sup>, Magdy S. Amer<sup>2</sup>, Neveen A. Salem<sup>3</sup>, Hebatullah M. Abou El-Fadl<sup>2</sup>**

<sup>1</sup>Hormones Department, National Research Centre, Dokki, Cairo, Egypt.

<sup>2</sup>Pharmacology Department, Faculty of Veterinary Medicine, Mansoura University,  
Mansoura, Egypt.

<sup>3</sup>Narcotics, Ergogenic Aids and Poisons Department, National Research Centre, Dokki,  
Cairo, Egypt.

Article Received on  
24 August 2013,

Revised on 28 Sept. 2013,  
Accepted on 30 October 2013

**\*Correspondence for  
Author:**

**Dr. Hanaa H. Ahmed**

Hormones Department,  
National Research Centre,  
Dokki, Cairo, Egypt.

[hanaaomr@yahoo.com](mailto:hanaaomr@yahoo.com)

### **ABSTRACT**

This study aimed at evaluating the therapeutic role of bone marrow derived mesenchymal stem cells (BM-MSCs) in management of liver fibrosis in rats. The MSCs were harvested from bone marrow of male albino rats. The isolated BM-MSCs proved their MSCs identity *via* their morphological appearance, multilineage potential and positive expression for CD29, CD44 as well as CD106 and negative expression for CD14, CD34 and CD45. Forty adult female albino rats were used in the present study and classified as follows: group (1) negative control, group (2) positive control (TAA), group (3) TAA+DMEM and group (4) TAA+ BM-MSCs. Circulating values of AST, ALT, ammonia, albumin, fibronectin and fibrinogen were estimated. Hepatic

TGF- $\beta$  and HGF contents were determined. Histological investigation of liver tissue was carried out. The engraftment of PKH-stained undifferentiated BM-MSCs in the liver of TAA group confirms the homing of BM-MSCs to the injured liver. Treatment with BM-MSCs resulted in significant improvement in liver functions associated with significant reduction in serum fibronectin level. Moreover, hepatic TGF- $\beta$  was significantly downregulated and HGF was remarkably upregulated in BM-MSCs treated group. Histological examination of liver tissue documented the biochemical results. In conclusion, the present results spotlight on the good influence of BM-MSCs in the treatment of experimental liver fibrosis and pave the way for the therapeutic application of BM-MSCs against human liver fibrosis.

**Key Words:** liver fibrosis, bone marrow mesenchymal stem cells, therapeutic application, rats.

## 1. INTRODUCTION

Liver fibrosis is the wound-healing response of the liver to chronic injury; the liver undergoes tissue remodeling and forms fibrosis, which is characterized by excessive accumulation of extracellular matrix, with the formation of scar tissue encapsulating the area of injury. This leads to many clinical manifestations, including ascites, variceal hemorrhage and encephalopathy. The onset of liver fibrosis is usually insidious, and most of the related morbidity and mortality occur after the development of cirrhosis.<sup>[1]</sup> In the majority of patients, progression to cirrhosis occurs after an interval of 15–20 years. Patients with cirrhosis can remain free of major complications for several years (compensated cirrhosis). While, decompensated cirrhosis is associated with short survival.<sup>[2]</sup> Currently, there is no standard treatment for liver fibrosis and liver transplantation remains a good alternative treatment. However, there are limited available donor livers for the hundreds of millions of patients worldwide. Thus, it is very important to investigate appropriate therapies and different treatments for this disease.<sup>[3]</sup>

Although experimental studies have revealed targets to prevent fibrosis progression in rodents; the efficacy of most treatments has not been proven in humans.<sup>[4]</sup> This is due to the need to perform serial liver biopsies to accurately assess changes in liver fibrosis. Thus, there is considerable drive to develop improved therapies for liver fibrosis, thereby reducing morbidity, mortality, and the overall economic impact associated with this condition. Such an ambition lies beyond the reach of conventional medicine, with its mainly monofactorial approach to the treatment of the diseases.<sup>[5]</sup>

Cell therapy can be defined as the use of living cell to restore, maintain or enhance the function of tissues and organs.<sup>[6]</sup> Stem cells are unspecialized cells that can self-renew indefinitely and can also differentiate into more mature cells with specialized functions. They are cells that have the ability to divide (self-replicate) for indefinite periods often throughout the life of the organism. Under the right conditions, or given the right signals, stem cells can give rise (differentiate) to the many different cell types that make up the organism. These, stem cells have the potential to develop into mature cells that have characteristic shapes and specialized functions, such as heart cells, skin cells, nerve cells and liver cells.<sup>[7]</sup>

The present study was designed to elucidate the possible therapeutic role of bone marrow mesenchymal stem cells (BM-MSCs) in management of liver fibrosis in rat model.

## 2. MATERIALS AND METHODS

### *I. Isolation and preparation of BM-MSCs*

Bone marrow stem cells were harvested by flushing the tibiae and femurs of 12-week-old male *albino* rats with Dulbecco's modified Eagle's medium (DMEM, GIBCO/BRL, Grand Island, New York, USA) supplemented with 10% fetal bovine serum (GIBCO/BRL). Nucleated cells were isolated with a density gradient [Ficoll/Paque (Pharmacia)] and resuspended in complete culture medium supplemented with 1% penicillin–streptomycin (GIBCO/BRL). Cells were incubated at 37 °C in 5% humidified CO<sub>2</sub> for 12–14 days as primary culture or upon formation of large colonies. When large colonies developed (80–90% confluence), cultures were washed twice with phosphate buffer saline (PBS) and the cells were trypsinized with 0.25% trypsin in 1mM EDTA (GIBCO/BRL) for 5 min at 37 °C. After centrifugation, cells were resuspended with serum-supplemented medium and incubated in 50 cm<sup>2</sup> culture flask (Falcon). These cultures were referred to as first-passage cultures.<sup>[8]</sup> To ensure that the cells in culture are MSCs, they were characterized morphologically by inverted microscope examination. Also, multilineage potential of BM-MSCs was confirmed *via in vitro* differentiation to adipocytes, chondrocytes and osteocytes. Additionally, PCR detection of CD14, CD29, CD34, CD44, CD45 and CD106 gene expression was done.

### *II. In vitro differentiation of BM-MSCs*

Bone marrow derived cells were grown until confluence and the growth medium was replaced with the inductive medium consisting of Iscove's modified Dulbecco's medium (INVITROGEN, USA), 20% fetal calf serum, 100 U/mL penicillin, 100 µg/mL streptomycin and 0.05 mM β-mercaptoethanol supplemented with specific differentiation reagents as follows:

#### **a) Adipogenesis assay**

Cells were incubated for 3 weeks with 5 µg/mL insulin (SIGMA, USA) and 10<sup>-9</sup> M dexamethasone. Adipogenic differentiation was visualized in phase-contrast microscopy by the presence of highly refractive intracellular lipid vacuoles.<sup>[9]</sup> Oil Red O (SIGMA, USA) staining was used to assay the accumulation of lipid droplets in these vacuoles.

**b) Chondrogenesis assay**

The cells were harvested and  $6 \times 10^5$  cells were centrifuged to form a pellet on the bottom of a 15 mL polypropylene tube (Falcon). The micromass was cultured in 500  $\mu$ L of chondrogenic medium that consisted of 50  $\mu$ g/mL ascorbic acid 2-phosphate and 1 ng/mL TGF- $\beta$ 1 (SIGMA, USA).<sup>[10]</sup> After 3 weeks of culture, cell clumps were harvested, embedded in paraffin, cut into 3 $\mu$ m sections, and stained for glycosaminoglycans using 0.1% Alcian blue (SIGMA, USA).

**c) Osteogenesis assay**

Cultures were fed twice a week for 3 weeks with 10 mM  $\beta$ -glycerophosphate, 50  $\mu$ g/mL ascorbic acid 2-phosphates and  $10^{-9}$  M dexamethasone.<sup>[11]</sup> Then cells were fixed with 10% formalin for 20 min at room temperature and mineralization (presence of calcium-rich hydroxyapatite) of the extracellular matrix was assessed by staining for 20 min with 2% wt/vol Alizarin Red S, adjusted to pH 4.1 with ammonium hydroxide (all reagents were obtained from SIGMA, USA).

**III. PCR detection of CD14, CD29, CD34, CD44, CD45 and CD106 genes expression**

In order to confirm that the isolated cells from bone marrow are mesenchymal stem cells, total RNA was extracted from cultured cells using RNeasy mini kit for purification of total RNA from animal cells (QIAGEN, Germany) according to the manufacturer's instructions. Then, the reverse transcription of the extracted RNA (1  $\mu$ g) was carried out using the high capacity cDNA reverse transcription kit (APPLIED BIOSYSTEMS, USA) according to the manufacturer's instructions.

**Conventional PCR detection of CD29, CD34 and CD45 gene expression**

The conventional PCR reaction mix for CD29, CD34 and CD45 was 12.5  $\mu$ L of master mix (QIAGEN, Germany), 1  $\mu$ L of the corresponding forward primer (10 pmol/ $\mu$ L), 1  $\mu$ L of the corresponding reverse primer (10 pmol/ $\mu$ L) (INVITROGEN, USA) (**Table 1**), 5  $\mu$ L cDNA and 5.5  $\mu$ L nuclease free water. PCR was performed using the thermal cycler instrument, Biometra T professional, (USA) for 35 cycles with initial denaturation step at 94°C for 3 min for CD29 as well as CD45 and for 2 min for CD34. Each cycle consisted of denaturation at 94 °C for 30 s, annealing at 57 °C for CD29 as well as CD45 and at 55°C for CD34 for 30 s, elongation at 72 °C for 1 min followed by 7 min of terminal extension at 72 °C after completion of the last cycle. The PCR product was separated by electrophoresis through a 1% agarose gel, stained, and photographed under ultraviolet light.

**Real time PCR detection of CD14, CD44 and CD106 gene expression**

The real time PCR was performed using the QuantiTect SYBR green PCR Kit (QIAGEN, Germany) by Applied Biosystems 7500 Instrument, USA. The real time PCR reaction mix was carried out in a total volume of 25  $\mu$ L, containing 12.5  $\mu$ L of 2 x QuantiTect SYBR green PCR master mix, 0.5  $\mu$ L of forward primer for GAPDH (20 pmol/ $\mu$ L), 0.5  $\mu$ L of reverse primer for GAPDH (20 pmol/ $\mu$ L) (**Table 1**), 4  $\mu$ L cDNA and 7.5  $\mu$ L nuclease free water. The real time PCR reaction mix for CD14 was 12.5  $\mu$ L of 2 x QuantiTect SYBR green PCR master mix, 1  $\mu$ L of forward primer (10 pmol/ $\mu$ L), 1  $\mu$ L of reverse primer (10 pmol/ $\mu$ L) (**Table 1**), 4  $\mu$ L cDNA and 6.5  $\mu$ L nuclease free water. While, the reaction mix for CD44 and CD106 were 12.5  $\mu$ L of 2 x QuantiTect SYBR green PCR master mix, 1  $\mu$ L of the corresponding forward primer (10 pmol/ $\mu$ L), 1  $\mu$ L of the corresponding reverse primer (10 pmol/ $\mu$ L) (**Table 1**), 3  $\mu$ L cDNA and 7.5  $\mu$ L nuclease free water. The protocol consisted of 45 amplification cycles, each conducted as follows: 10 min at 95°C (holding stage), 15 sec for denaturation at 95°C, 30 sec for annealing at 60°C and finally, 15 sec for extension at 60°C.

**Table (1): Primer sequences of the tested genes.**

Genes	Forward (5'-3')	Reverse (5'-3')	References
<b>CD14</b>	GTGTGAGTGGTAGCCAGCAA	TGCGCAGCGCTAAACTTG	Schäfer et al. <sup>[12]</sup>
<b>CD29</b>	AATGTTTCAGTGCAG AGC	TTGGGATGATGTCGGGAC	Wang et al. <sup>[13]</sup>
<b>CD34</b>	GCCCAGTCTGAGGTTAGGCC	ATTGGCCTTTCCCTGAGTCT	Qin et al. <sup>[14]</sup>
<b>CD44</b>	TTGGCATCCCTCCTGGCGCTGG	AAGGAGGAACTGGAAGAGACCC	Qin et al. <sup>[14]</sup>
<b>CD45</b>	ACCAGGGGTTGAAAAGTTTCAG	GGGATTCCAGGTAATTACTCC	Muñoz-Fernández et al. <sup>[15]</sup>
<b>CD106</b>	CCTCACTTGCAGCACTACGGGCT	TTTTC CAATATCCTCAATGACGGG	Lau and Bhatia <sup>[16]</sup>
<b>GAPDH</b>	CAAGGTCATCCATGACAACTTTG	GTCCACCACCCTGTTGCTGTAG	Schäfer et al. <sup>[12]</sup>

#### IV. Labeling of mesenchymal stem cells with PKH26 dye

The cells were harvested during the 1<sup>st</sup> passage and labeled with PKH26 (SIGMA-ALDRICH, USA) fluorescent linker dye. PKH26 is a red fluorochrome that has excitation (551 nm) and emission (567 nm) wavelengths. The linkers are physiologically stable and show little to no toxic side-effects on cell systems. Labeled cells retain both biological and proliferating activity, and are ideal for *in vitro* cell labelling, *in vitro* proliferation studies and long term, *in vivo* cell tracking. Labeled cells that have been washed can be visualized in culture up to 100 days after staining (for non-dividing cells). This enhanced stability is favorable for long term *in vivo* studies. The dye itself is stable and it divides equally when the cells divide. After staining with PKH dye, one can observe as many as 8 divisions depending on how brightly the cells were stained initially and the amount of surface area on the cells. Most commonly, 4-6 divisions can be visualized.

Final concentrations of  $2 \times 10^{-6}$  M PKH26 dye and  $1 \times 10^7$  cells/ml in a 2 ml total volume was stained according the following manufacturer's instructions: adherent or bound cells were removed using proteolytic enzymes (i.e., trypsin) and put into a single cell suspension. All steps were performed at 25 °C. A total volume of approximately  $2 \times 10^7$  single cells was placed in a conical bottom polypropylene tube and washed once using culture medium without serum. Then, the cells were centrifuged (400 x g) for 5 minutes into a loose pellet. After centrifuging cells, the supernatant was carefully aspirated leaving no more than 25 ml of supernatant on the pellet. Then, 1 ml of diluent C (supplied with the kit) was added and cells were resuspended, then pipetting was done to insure complete dispersion. Immediately prior to staining,  $4 \times 10^{-6}$  M PKH26 dye was prepared (this was a 2X stock) in polypropylene tubes using diluent C.

To minimize ethanol effects, the amount of dye added was less than 1% of the individual sample volume. The 1 ml of 2X cells was rapidly added to 1 ml of 2X dye and the sample was immediately mixed by pipetting (rapid and homogeneous mixing was critical for uniform labeling because staining is nearly instantaneous). The sample was incubated at 25 °C for 2 to 5 minutes. The tube was periodically inverted gently to assure mixing during this staining period at 25 °C. Then, the staining reaction was stopped by adding an equal volume of serum and incubated for 1 min. The serum-stopped sample was diluted with an equal volume of complete medium (not diluent C). The cells were centrifuged at 400 x g for 10 min. at 25 °C to remove cells from staining solution. The supernatant was removed and the cell pellet was

transferred to a new tube for further washing (a minimum of 3 washes was recommended). 10 ml of complete culture medium was added to wash the cells, then the cells were centrifuged and resuspended to the desired concentration. Finally, the cells were examined using fluorescence microscopy.

#### V. *Experimental animals*

Forty adult female *albino* rats weighing 130-150 g were obtained from the Animal House Colony of the National Research Centre, Cairo, Egypt and acclimatized in a specific area where temperature  $25\pm1^{\circ}\text{C}$  and humidity 55%. Rats were controlled constantly with a 12 hrs light/dark cycles at National Research Centre Animal Facility Breeding Colony. Rats were individually housed with *ad libitum* access to standard laboratory diet consisted of casein 10%, salt mixture 4%, vitamin mixture 1%, corn oil 10% and cellulose 5% and then completed to 100 g with corn starch and tap water. All animals received human care and use according to the guidelines for Animal Experiments which were approved by the Ethical Committee of Medical Research, National Research Centre, Egypt.

The animals were classified into 4 groups (10 rats/group). The first group was healthy control group (Negative control group). The groups from second to fourth were injected intraperitoneally (i.p) with thioacetamide (SIGMA, USA) in a dose of 100 mg/kg b.wt three times weekly for 6 weeks<sup>[17]</sup> to induce liver fibrosis. The second group was left untreated and served as positive control group (TAA). The third group was injected with 0.5 ml culture media alone into the tail vein (i.v). The fourth group was injected with 0.5 ml of culture media containing  $3\times 10^6$  BM-MSCs intravenously.<sup>[18]</sup> As the liver fibrosis induced rats were deeply anaesthetized and the cells were suspended in 100  $\mu\text{l}$  PBS before transplantation and then slowly injected into the tail vein in 5 min with a 27G needle. The needle was kept in the tail vein for another 5 min to avoid regurgitation and then withdrawn.

At the end of the experimental period (after one month from cells transplantation), animals were fasted for 12 hs and sacrificed. Then the blood and liver samples were collected from each rat. The liver samples were fixed in formalin saline (10%) for histological investigation.

#### VI. *Biochemical assays*

Serum aspartate aminotransferase (AST) and alanine aminotransferase (ALT) activities were estimated by kinetic method using kit purchased from QUIMICA CLINICA APLICADA S.A. Co., Spain, according to the method of Bergmeyer.<sup>[19]</sup> Ammonia level was determined in



plasma by enzymatic UV method using kit purchased from RANDOX, UK, according to the method of Mondzac et al.<sup>[20]</sup> Serum albumin was measured by quantitative colorimetric method using kit purchased from STANBIO Laboratory Boerne, Texas, USA, according to the method described by Young et al.<sup>[21]</sup>

Plasma fibrinogen (FBG) level was estimated by ELISA technique using kit purchased from ASSAYPRO, USA., according to the method of Handley and Hughes.<sup>[22]</sup> Serum fibronectin level was detected by ELISA using kit purchased from ASSAYPRO, USA, according to the method of Wu et al.<sup>[23]</sup> Hepatic hepatocyte growth factor (HGF) content was determined by ELISA technique using the kit purchased from GLORY Science Co., USA according to the method described by Miyazawa et al.<sup>[24]</sup> Hepatic transforming growth factor  $\beta$ 1 (TGF- $\beta$ 1) content was assayed by ELISA using TGF- $\beta$ 1 kit purchased from GLORY Science, USA, according to the manufacturer's instructions . Quantitative estimation of total protein content in the liver was carried out according to the method of Lowry et al.<sup>[25]</sup> to express the concentration of HGF and TGF- $\beta$ 1 in the liver per milligram protein.

#### ***VII. Histopathological investigation***

After fixation of liver samples of the rats in the different groups in 10% formalin saline for 24 hours, washing was done in tap water then, serial dilutions of alcohol (methyl, ethyl and absolute ethyl) were used for dehydration. Specimens were cleared in xylene and embedded in paraffin wax at 56 degree in hot air oven for 24 hours. Paraffin blocks were prepared for sectioning at 4 microns by sledge microtome. The obtained tissue sections were collected on glass slides, deparaffinized and stained by hematoxylin and eosin stains<sup>[26]</sup> for histopathological examination through the light microscope.

#### ***VIII. Statistical analysis***

In the present study, all results were expressed as Mean  $\pm$  S.E of the mean. Data were analyzed by one way analysis of variance (ANOVA) using the Statistical Package for the Social Sciences (SPSS) program, version 14 followed by least significant difference (LSD) to compare significance between groups.<sup>[27]</sup> Difference was considered significant when P value was  $< 0.05$ .



### 3. RESULTS

#### *I. Stem cells morphology*

The photomicrograph in "Fig. 1a" shows the spindle shape of cells which is the typical morphological aspects of mesenchymal stem cells derived from bone marrow through culture flask at day 14.

#### *II. In vitro differentiation of BM-MSCs*

##### **a) Adipogenic differentiation**

Bone marrow stem cells are differentiated into adipocytes through 1 week of the addition of inductive media. Meanwhile, after 2 weeks, the number of adipocytes increased. The differentiation into adipocytes is indicated by staining with Oil Red O stain "Fig. 1b".

##### **b) Chondrogenic differentiation**

Bone marrow stem cells are differentiated through 1 week of addition of inductive media into chondrocytes, as indicated by their round configuration and the development of an extracellular matrix that stained with special Alcian blue stain "Fig.1c".

##### **c) Osteogenic differentiation**

Bone marrow stem cells are differentiated into osteocytes through 1 week of the addition of inductive media "Fig.1d". The osteocytes are visualized by staining with special Alizarin Red S stain.

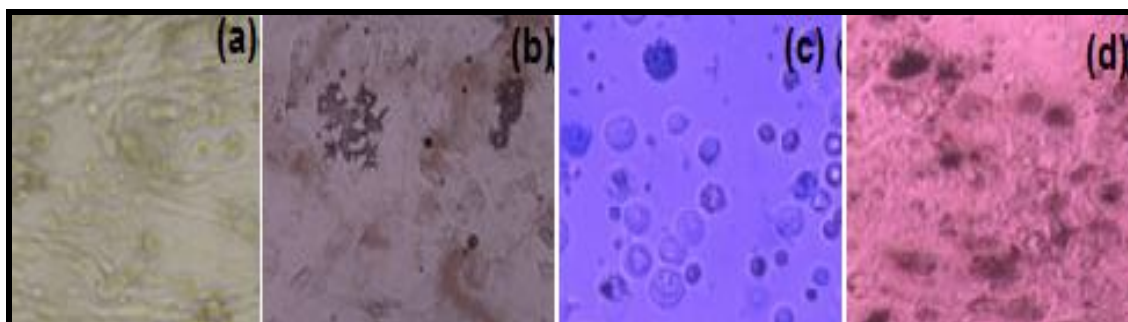


**Fig. 1: Morphological aspects and *in vitro* differentiation of isolated BM-MSCs. (a):**

Morphological aspect (spindle shape) of mesenchymal stem cells derived from bone marrow through culture flask at day 14; (b): Differentiation of BM-MSCs into adipocytes after addition of inductive media and staining with special Oil Red O stain; (c): Differentiation of BM-MSCs into chondrocytes after addition of inductive media and staining with special

Alcian blue stain; (d): Differentiation of BM-MSCs into osteocytes after addition of inductive media and staining with special Alizarin Red S stain.

### III. Cell surface markers genes expression

The agarose gel electrophoresis showed that the BM-derived stem cells used in the present study are positive for CD29, a cell surface marker for MSCs as indicated by the positive band appears at 261 bp "Fig. 2", and negative for CD45 as well as CD34 which are cell surface markers associated with hematopoietic precursor cells and endothelial cells "Fig. 2" and "Fig. 3" respectively.



**Fig. 2: Agarose gel electrophoresis for CD29 and CD45 gene expression for BM-derived stem cells sample.** Lane (1) represented DNA ladder, lane (2) represented CD29 gene expression and lane (3) represented CD45 gene expression.

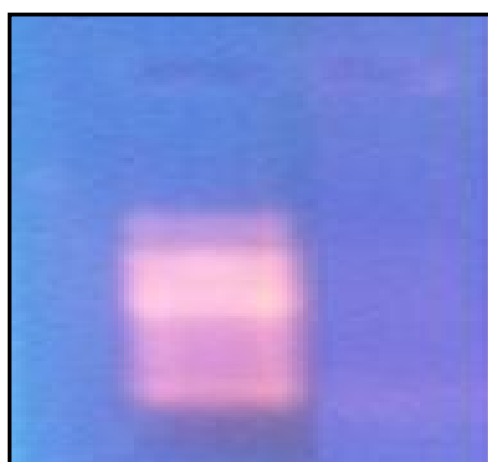


**Fig. 3: Agarose gel electrophoresis for CD34 gene expression for BM-derived stem cells sample.** Lane (1) represented DNA ladder, lane (2) represented CD34 gene expression.

Moreover, the amplification plots of the real time PCR for CD14, CD44 and CD106 showed that the used BM-derived stem cells are negative for CD14 gene expression, a cell surface marker associated with hematopoietic precursor cells "Fig. 4" and positive for CD44 as well as CD106 genes expression, cell surface markers for MSCs "Fig. 5". It is obvious from Fig. "5" that the expressions of CD44 and CD106 exceed the threshold of the linear phase of the real time PCR reaction which equal 1.733 and 2.313 respectively.

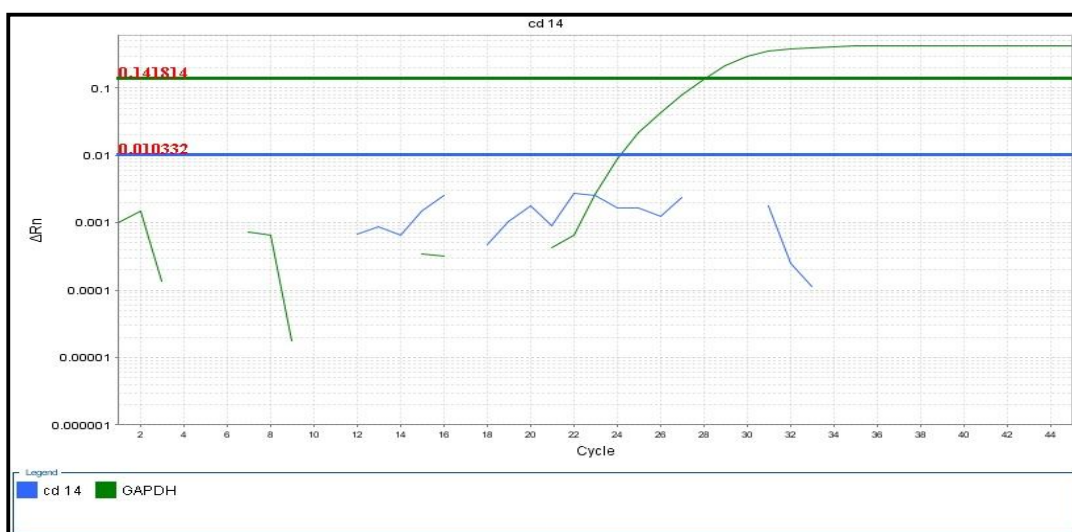


**Fig. 4:** The real time PCR amplification plot for CD14 gene expression for the BM-derived stem cells sample.

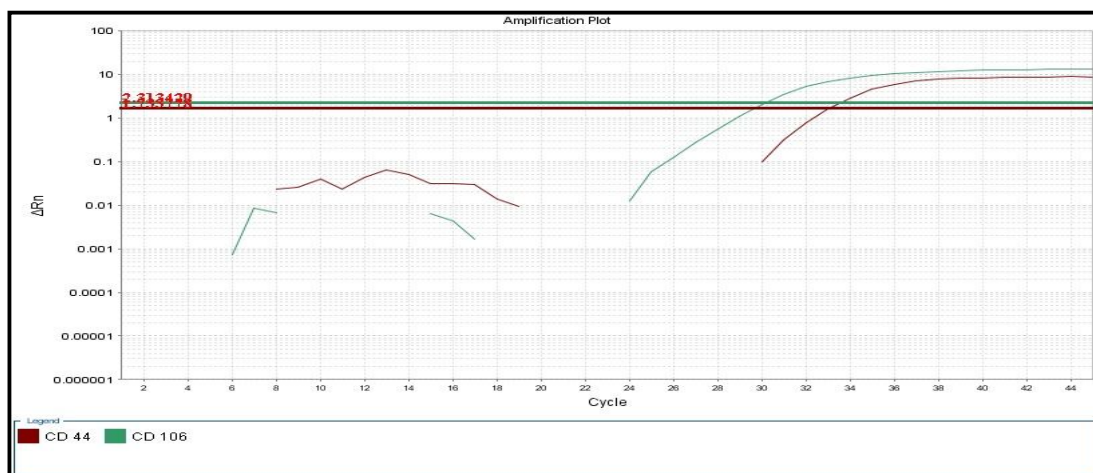


**Fig. 5:** The real time PCR amplification plot for CD44 and CD106 genes expression for the BM-derived stem cells sample.

#### IV. Mesenchymal stem cells homing

The engraftment of PKH-stained undifferentiated bone marrow derived mesenchymal stem cells (BM-MSCs) in the liver of thioacetamide administered rats as shown in Fig. "6" indicated that the systemically delivered single dose of undifferentiated MSCs is able to home at the injured liver.

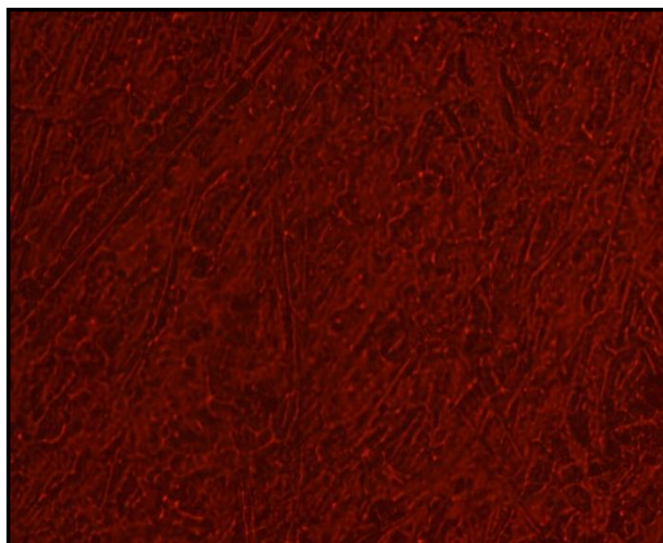


**Fig. 6: Engraftment of PKH-stained undifferentiated BM-MCs in thioacetamide-injured rat liver.**

#### ***V. Biochemical results***

The data in **Table (2)** show the effect of treatment with BM-MSCs on serum AST and ALT activities as indicators for liver functions as well as on plasma ammonia and serum albumin levels in rats bearing liver fibrosis. The untreated thioacetamide (TAA) administered group shows significant increase ( $P < 0.05$ ) in serum AST and ALT activities as well as in plasma ammonia level associated with significant decrease ( $P < 0.05$ ) in serum albumin level as compared to the negative control group. The group of rats infused with DMEM shows insignificant change ( $P > 0.05$ ) in serum AST and ALT activities as well as in plasma ammonia and serum albumin levels when compared with the untreated thioacetamide administered group.

In the case of treatment of thioacetamide administered rats with undifferentiated BM-MSCs, significant decrease ( $P < 0.05$ ) in serum AST and ALT activities as well as in plasma ammonia level is recorded as compared to both the untreated thioacetamide administered and DMEM infused groups. On the other hand, treatment with BM-MSCs causes significant increase ( $P < 0.05$ ) in serum albumin level in comparison with the untreated thioacetamide administered group. Insignificant increase ( $p > 0.05$ ) in serum albumin level was detected in BM-MSCs treated group when compared with DMEM infused group.

**Table (2): Effect of treatment with BM-MSCs on serum AST and ALT activities as well as plasma ammonia and serum albumin levels in rats bearing liver fibrosis. Data are represented as Mean  $\pm$  S.E of 10 rats/group.**

Groups	AST (U/L)	ALT (U/L)	Ammonia ( $\mu$ mol/L)	Albumin (g/dL)
Negative control	42.2 $\pm$ 0.6	26.6 $\pm$ 0.2	366.0 $\pm$ 30.2	3.90 $\pm$ 0.1
Positive control (TAA)	83.6 $\pm$ 1.0 <sup>a</sup>	60.5 $\pm$ 0.7 <sup>a</sup>	631.0 $\pm$ 57.2 <sup>a</sup>	2.90 $\pm$ 0.2 <sup>a</sup>
TAA + DMEM	79.9 $\pm$ 2.2	59.9 $\pm$ 0.5	606.0 $\pm$ 30.4	2.98 $\pm$ 0.1
TAA + BM-MSCs	56.0 $\pm$ 2.4 <sup>bc</sup>	38.3 $\pm$ 0.7 <sup>bc</sup>	383.0 $\pm$ 6.8 <sup>bc</sup>	3.30 $\pm$ 0.2 <sup>b</sup>

Where a, b and c represent the significant change at  $P < 0.05$  in comparison with –ve control group, the thioacetamide untreated group and the TAA + DMEM group respectively.

**Table (3)** shows the effect of treatment with BM-MSCs on serum fibronectin and plasma fibrinogen levels in rats bearing liver fibrosis. The untreated thioacetamide administered group shows significant increase ( $P < 0.05$ ) in serum fibronectin level accompanied with significant decrease ( $P < 0.05$ ) in plasma fibrinogen level in comparison with the negative control group. Infusion of thioacetamide administered rats with DMEM produces insignificant change ( $P > 0.05$ ) in the circulating levels of fibronectin and fibrinogen when compared with the untreated thioacetamide administered group. While, the treatment with BM-MSCs results in significant decrease ( $P < 0.05$ ) in serum fibronectin level in concomitant with significant increase ( $P < 0.05$ ) in plasma fibrinogen level in comparison with both untreated thioacetamide administered and DMEM infused groups.

**Table (3): Effect of treatment with BM-MSCs on serum fibronectin and plasma fibrinogen levels in rats bearing liver fibrosis. Data are represented as Mean  $\pm$  S.E of 10 rats/group.**

Groups	Fibronectin ( $\mu$ g/mL)	Fibrinogen ( $\mu$ g/mL)
Negative control	921 $\pm$ 10.3	2464 $\pm$ 77.8
Positive control (TAA)	1606 $\pm$ 21.1 <sup>a</sup>	1390 $\pm$ 20.0 <sup>a</sup>
TAA + DMEM	1592 $\pm$ 6.9	1400 $\pm$ 61.2
TAA + BM-MSCs	1112 $\pm$ 20.2 <sup>bc</sup>	2366 $\pm$ 13.9 <sup>bc</sup>

Where a, b and c represent the significant change at  $P < 0.05$  in comparison with –ve control group, the thioacetamide untreated group and the TAA + DMEM group respectively.

The results in **Table (4)** show the effect of treatment with BM-MSCs on hepatic transforming growth factor  $\beta$  (TGF- $\beta$ ) and hepatocyte growth factor (HGF) contents in rats bearing liver fibrosis. The untreated thioacetamide administered group reveals significant increase ( $P < 0.05$ ) in hepatic TGF- $\beta$  content associated with insignificant increase ( $P > 0.05$ ) in hepatic HGF content in comparison with the negative control group. The group of rats infused with DMEM shows insignificant change ( $P > 0.05$ ) in hepatic content of each of TGF- $\beta$  and HGF when compared with the untreated thioacetamide administered group. Treatment with BM-MSCs causes significant decrease ( $P < 0.05$ ) in hepatic TGF- $\beta$  content in comparison with the untreated thioacetamide administered group as well as DMEM infused group. In comparison with the untreated thioacetamide administered group, treatment with BM-MSCs produces insignificant increase ( $P > 0.05$ ) in hepatic HGF content, while in comparison with DMEM infused group, the treatment with BM-MSCs results in significant increase ( $P < 0.05$ ) in hepatic HGF content.

**Table (4): Effect of treatment with BM-MSCs on hepatic TGF- $\beta$  and HGF contents in rats bearing liver fibrosis. Data are represented as Mean  $\pm$  S.E of 10 rats/group.**

Groups	TGF- $\beta$ (ng/mg protein)	HGF (ng/mg protein)
Negative control	7.5 $\pm$ 0.6	12.4 $\pm$ 0.4
Positive control (TAA)	35.9 $\pm$ 3.2 <sup>a</sup>	15.5 $\pm$ 1.0
TAA + DMEM	32.3 $\pm$ 2.0	14.7 $\pm$ 0.9
TAA + BM-MSCs	24.5 $\pm$ 1.9 <sup>bc</sup>	18.5 $\pm$ 0.9 <sup>c</sup>

Where *a*, *b* and *c* represent the significant change at  $P < 0.05$  in comparison with –ve control group, the thioacetamide untreated group and the TAA + DMEM group respectively.

#### **VI. Histopathological results**

Microscopic investigation of liver tissue section of negative control group shows normal histological structure of the portal area and the surrounding hepatocytes "Fig.7a,b". While, the photomicrographs of liver tissue section of the group administered with thioacetamide and left untreated show that the portal area displayed sever congestion in the portal vein with infiltrate of inflammatory cells as well as fibroblastic cells proliferation which were extended



in between the hepatocytes dividing the parenchyma into lobules "Fig. 8a,b". Also, brown pigments were detected in the portal area of the liver of TAA administered rat "Fig. 9" indicating the state of hepatocellular cholestasis. The photomicrographs of the liver tissue section of the group of rats administered with thioacetamide and infused with DMEM (TAA + DMEM) show that the portal area exhibited sever congestion in the portal vein with inflammatory cells and fibrosis which extended between the hepatocytes and divided the hepatic parenchyma into lobules "Fig. 10a,b". In addition to, newly formed proliferated dysplastic bile ductules in the portal area associated with inflammatory cells infiltration and fibrosis in between "Fig. 11a,b,c". The photomicrographs of the liver tissue section of the group of rats administrated with thioacetamide and treated with BM-MSCs (TAA+ BM-MSCs) show infiltrate of inflammatory cells in the focal manner at the portal area and in diffuse manner between the hepatocytes "Fig.12a,b,c".

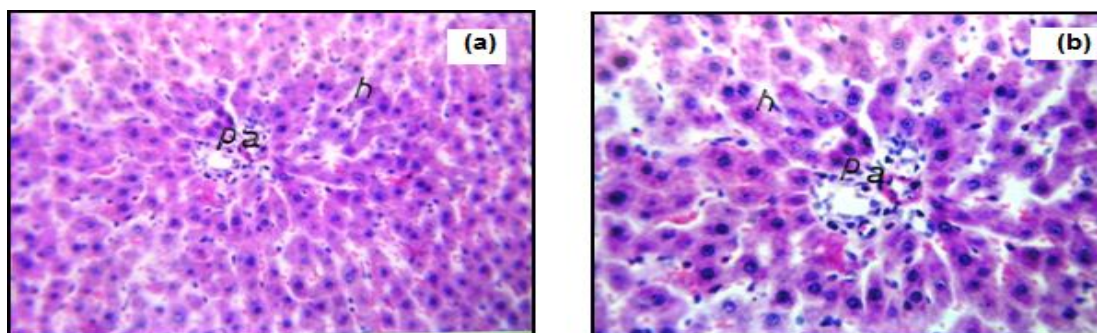


**Fig. 7: Photomicrographs of liver tissue section of negative control rat.** (a): shows the normal histological structure of the portal area (pa) and surrounding hepatocytes (H & E x 64). (b): shows the magnification of Fig. (7a) to identify the normal histological structure of the portal area (pa) and the surrounding hepatocytes (H & E x 80).

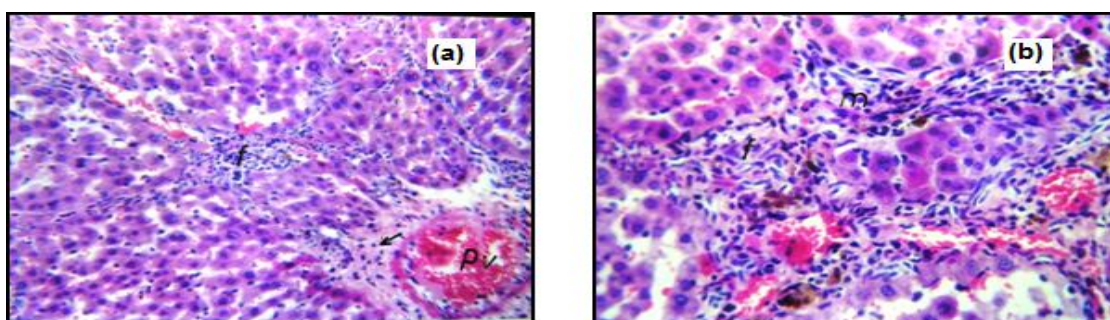


**Fig. 8: Photomicrographs of liver tissue section of thioacetamide administered rat.** (a): shows sever congestion in the portal vein (pv) with inflammatory cells (arrow) infiltration in portal area (H&E x 64). (b): shows fibrosis (f) and inflammatory cells infiltration (m) originating from portal area and dividing the parenchyma into lobules (H&E x 80).)



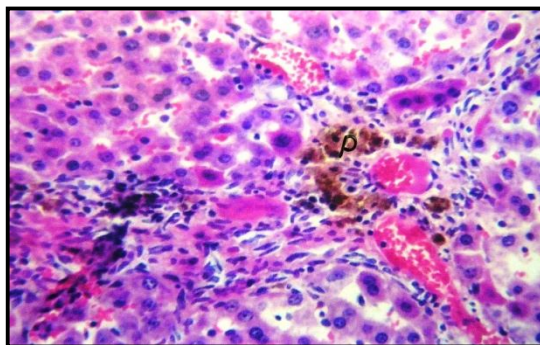


**Fig. 9: Photomicrograph of liver tissue section of thioacetamide administered rat shows brown pigment in the portal area (p) (H & E x 80).**

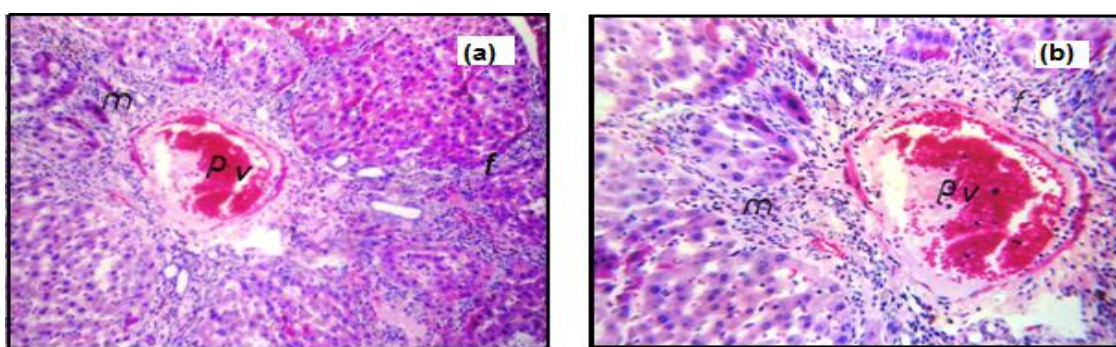


**Fig. 10: Photomicrographs of liver tissue section of rat from TAA + DMEM group. (a):** shows sever congestion in the portal vein (pv) with inflammatory cells (m) and fibrosis (f) in the portal area that extended between the hepatocytes to divide the hepatic parenchyma into lobules (H & E x 40). **(b):** shows the magnification of **Fig. (10a)** to identify the sever congestion in the portal vein (pv) and the fibrosis (f) with inflammatory cells infiltration (m) in the portal area (H & E x 64).

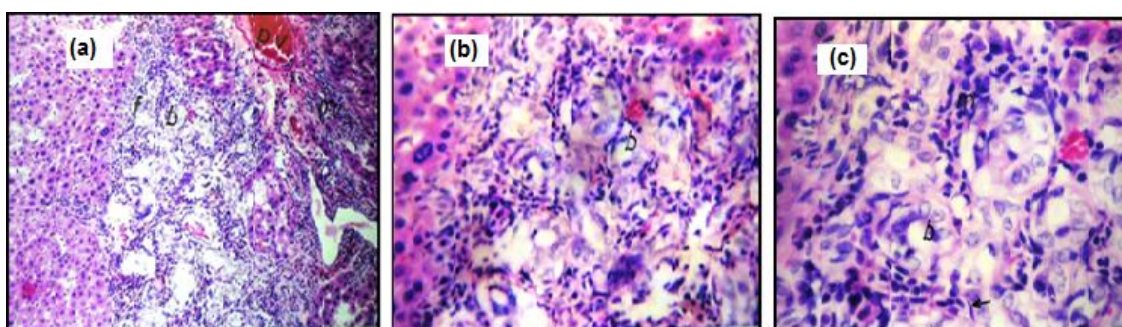


**Fig. 11: Photomicrographs of liver tissue section of rat from TAA + DMEM group. (a):** shows newly formed proliferated dysplastic bile ductules (b) associated with fibrosis and inflammatory cells infiltration in between (H & E x 40). **(b):** shows the magnification of **Fig. (11a)** (H & E x 80). **(c):** shows the magnification of **Fig. (11b)** to identify the proliferated dysplastic bile ductules (b) with inflammatory cells (m) and fibrosis (arrow) in between (H & E x 160).

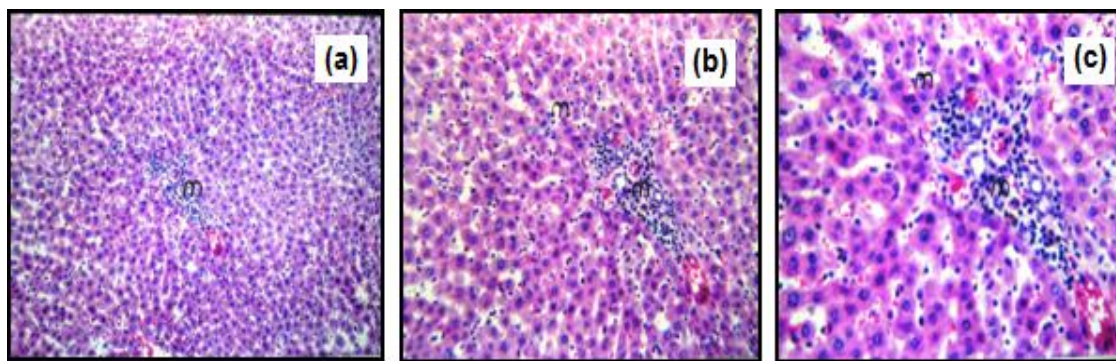


**Fig. 12: Photomicrographs of liver tissue section of rat from TAA + BM-MSCs group.** (a): shows focal inflammatory cells infiltration in the portal area (H & E x 40). (b): shows the magnification of **Fig. (12a)** to identify the focal inflammatory cells infiltration in the portal area (m) and in diffuse manner between the hepatocytes (H & E x 64). (c): shows the magnification of **Fig. (12b)** to identify the focal inflammatory cells infiltration in the portal area (m) (H & E x 80).

#### 4. DISCUSSION

Bone marrow mesenchymal stem cells were isolated from male rats to be used for management of liver fibrosis which was induced in female rats by thioacetamide administration. The confirmatory results for BM-MSCs properties indicated their adhesiveness and spindle shape in culture flask which are in agreement with those of Rochefort et al.<sup>[28]</sup> Also, the isolated BM-MSCs showed the ability to differentiate into adipocytes, chondrocytes and osteocytes as defined by Pittenger et al.<sup>[29]</sup> Moreover, the PCR results demonstrated that the isolated BM-MSCs were positive for CD29, CD44 as well as CD106 and negative for CD14, CD34 and CD45. These results are in accordance with those of Pittenger et al.<sup>[29]</sup> and Kumar et al.<sup>[30]</sup> As, cell homing and engraftment into the injured liver is an integral steps in cell-based therapies, PKH staining showed that obvious number of BM-MSCs were engrafted in the injured liver. The mechanism that governs the recruitment of MSCs is complicated and several signaling pathways,<sup>[31]</sup> growth factors and metalloproteinases<sup>[32]</sup> have been shown to contribute to the recruitment of stem cells in the injured liver. Wan et al.<sup>[33]</sup> demonstrated that TGF- $\beta$  is activated in vascular tissue in response to injury, and active TGF- $\beta$  stimulates the migration and homing of MSCs to the injured sites for vascular repair and remodeling. Thus, TGF- $\beta$  may act as an injury/stress-activated messenger to recruit MSCs for tissue repair, regeneration and pathological remodeling.<sup>[33]</sup>

In the assessment of liver damage by thioacetamide (TAA), the current data revealed that TAA administration produces significant increase in serum AST and ALT activities as well

as in plasma ammonia level associated with significant decrease in serum albumin level. These results indicate the induction of hepatocellular injury and liver dysfunction as a result of TAA administration. Attractive clues for increasing serum liver enzymes activity and the decreasing serum albumin level were greatly supported by the studies of Wang et al.<sup>[34]</sup> and Foo et al.<sup>[35]</sup> The elevation of serum AST and ALT activities are indicative of cellular leakage and loss of functional integrity of cell membrane in the liver<sup>[36]</sup> as the damage of liver cells due to thioacetamide administration causes leakage of cellular enzymes into serum. A decreased level of serum albumin is one of the analytical characteristics of human fibrosis.<sup>[37]</sup> Fontana et al.<sup>[38]</sup> reported that the hypoalbuminemia observed in rats with liver fibrosis could be not only due to the effect of thioacetamide administration on liver cells, but also due to the malnutrition and malabsorption associated with the disease.

In the same boat, it has been demonstrated that the increase in plasma ammonia level due to thioacetamide administration is in agreement with Chang et al.<sup>[39]</sup> and Mehul and Varsha.<sup>[40]</sup> Hyperammonemia in patients with chronic liver dysfunction is related to disturbances in the excretion and reutilization of ammonia. It has been suggested that impaired uptake of ammonia due to microcirculatory disturbances plays an important role in the impaired elimination of ammonia in patients with fibrosis.<sup>[41]</sup>

It is well documented that liver fibrosis is characterized by an excessive accumulation of extracellular matrix (ECM) components, which lead to the impairment of the hepatic function.<sup>[42]</sup> The ECM composition in fibrotic liver consists mainly of collagen types I and III and other noncollagenous proteins such as laminin and fibronectin.<sup>[43]</sup> Hepatic fibrogenesis results from an imbalance between enhanced connective tissue synthesis and diminished or altered matrix breakdown.<sup>[44]</sup> The first noticeable molecular change in the ECM after liver injury is fibronectin accumulation in the subsinusoidal space, followed by the synthesis, export and assembly of mature collagen fibrils and other ECM proteins, such as laminin.<sup>[45]</sup> In the present study, it has been recorded that, thioacetamide administration produces significant increase in serum fibronectin level. This result agrees with that of Perez et al.<sup>[42]</sup> and Park et al.<sup>[46]</sup> The former documented that TAA induced fibrogenesis is related to the modulation of ECM biosynthetic and degradative pathways.

The current data showed that thioacetamide administration produces significant decrease in plasma fibrinogen level. This finding is in agreement with Chang et al.<sup>[39]</sup> Fibrinogen is one



of the major acute phase proteins synthesized by the liver and its concentration is often used as a surrogate for systemic inflammation.<sup>[47]</sup> Aster<sup>[48]</sup> reported that low levels of fibrinogen among other coagulation proteins in fibrosis are classically ascribed to insufficient hepatic synthesis. In addition, the decrease in fibrinogen in liver fibrosis may occur due to the increase of fibrinogen degradation products.

Various cytokines and polypeptide growth factors are implicated in the pathogenesis of hepatic fibrosis/cirrhosis. Among the peptide mediators, TGF- $\beta$  is the profibrogenic master cytokine.<sup>[49]</sup> The overexpression of transforming growth factor- $\beta$  (TGF- $\beta$ ) is one predominant pathogenic cause for the development of hepatic fibrosis/cirrhosis. TGF- $\beta$  mediates liver fibrosis through autocrine and paracrine effects on various hepatic and infiltrating cell types.<sup>[50]</sup> This pathological process also involves major changes in the regulation of matrix degradation, in which plasminogen activator inhibitor 1 (PAI-1), a downstream effector of TGF- $\beta$  signaling, may be a key player.<sup>[51]</sup> TGF- $\beta$  markedly stimulates the expression of extracellular matrix components, including collagen, fibronectin and proteoglycans.<sup>[52]</sup> Considerable evidence has accumulated showing that excess expression of TGF- $\beta$  induces and orchestrates intracellular signaling events leading to increased matrix protein deposition and ultimately liver fibrosis.<sup>[53]</sup>

In the glow of the previous notion, our study revealed a marked increase in the liver content of TGF- $\beta$  in TAA administered group. This result agrees with Shek and Benyon<sup>[54]</sup> who reported that TGF- $\beta$  plays an essential role in tissue fibrogenesis. The free radicals resulting from TAA metabolism may activate myofibroblasts to produce growth factors.<sup>[55]</sup> TGF- $\beta$ 1 is a prominent profibrogenic cytokine with antiproliferative effects that can upregulate the deposition of ECM.<sup>[56]</sup> Schnur and his colleagues<sup>[57]</sup> reported that TGF- $\beta$  overexpression not only leads to more liver fibrosis while TAA was being administered but also leads to marked persistence of the fibrosis once TAA was discontinued. Moreover, Ling et al.<sup>[58]</sup> found that the degree of TAA induced lesions positively correlated with the expression of TGF- $\beta$  mRNA in the liver.

A slight increase in hepatic HGF content was observed in this study due to thioacetamide administration. HGF plays an important role in liver regeneration as an endocrine or paracrine factor. In the liver, HGF is synthesized by non parenchymal cells<sup>[59]</sup> and targets both parenchymal hepatocytes and bile duct epithelial cells. The signal-transducing receptor

for HGF is the c-met protooncogene product of transmembrane tyrosine kinase.<sup>[60]</sup> Matsumoto and Nakamura<sup>[59]</sup> reported that HGF mRNA and HGF activity increased in the liver of rats after various liver injuries.

Treatment with the mesenchymal stem cells isolated from bone marrow caused significant decrease in serum AST and ALT activities accompanied with significant increase in serum albumin level. This finding is greatly supported by that of Abdel Aziz et al.<sup>[61]</sup> who reported that treatment with BM-MSCs in CCl<sub>4</sub> induced liver fibrosis in rats leads to a decrease in serum ALT activity and an increase in serum albumin level.

Treatment with mesenchymal stem cells derived from bone marrow produced significant decrease in plasma ammonia associated with significant increase in plasma fibrinogen levels. Chang et al.<sup>[39]</sup> reported that transplantation of BM-MSCs results in a significant restoration of specific liver functions including ammonia metabolism and fibrinogen expression.

Changes in TAA-associated fibrosis induction and MSC-associated fibrosis resolution were assessed through the reduction in serum fibronectin level after treatment with mesenchymal stem cells from bone marrow. This finding fits with that of Hwang et al.<sup>[62]</sup> who used bone marrow mesenchymal stem cell in a rat model of thioacetamide-induced liver cirrhosis. It has been postulated that BM-MSCs may play a central role in ECM organization.<sup>[63]</sup>

In the present study, the treatment with bone marrow MSCs decreased hepatic TGF- $\beta$  content. The results of Sakaida<sup>[64]</sup> indicated a reduced mRNA expression of type I procollagen and TGF- $\beta$  in the liver one week after BM-MSCs infusion. Excessive TGF- $\beta$  activation is a major contributor to progressive fibrosis in many organs including lung, liver, kidney, heart, skin and arteries,<sup>[65]</sup> whereas sustained active TGF- $\beta$  released locally due to chronic repetitive tissue injury may cause aberrant excessive recruitment of stem/progenitor cells, leading to excessive accumulation of myofibroblasts and progressive fibrosis due to their subsequent differentiation. Therefore, the capability of BM-MSCs to overcome fibrosis leads to the downregulation of hepatic TGF- $\beta$  as shown in the present study.

The ability of MSCs derived from bone marrow to restore liver function and promote regeneration might be attributed to a variety of bioactive cytokines secreted by these cells, such as vascular endothelial growth factor (VEGF), HGF and fibroblast growth factor (FGF).<sup>[66,67]</sup> Stem cells may positively influence the recovery from tissue injury *via* paracrine

factors for neighboring parenchymal cells that promote tissue repair.<sup>[68]</sup> Our data revealed that the treatment with MSCs leads to an elevation in hepatic HGF content. It was reported that HGF could play a role in accelerating recovery of liver function. HGF may promote regeneration of damaged liver tissue through antiapoptotic effect by increasing hepatocyte proliferation, and through the mesenchymal-epithelial transition factor (c-met) signaling pathway.<sup>[69]</sup> Stimulation of c-met *via* its ligand hepatocyte growth factor also known as scatter factor (HGF/S), leads to a plethora of biological and biochemical effects in the cell.<sup>[70]</sup>

Secretion of HGF by MSCs leads to the apoptotic death of activated hepatic stellate cells (HSCs).<sup>[71]</sup> Oyagi et al.<sup>[72]</sup> reported that when BM-MSCs co-cultured with CCl<sub>4</sub>-injured hepatocytes, they secreted significantly higher concentration of HGF than that in the coculture with normal hepatocytes. These findings suggested that BM-MSCs appear to receive certain signal from injured hepatocytes and secrete HGF into the medium.

From the histological examination of liver tissue sections, it has been found that the administration of thioacetamide in rats three times weekly for 6 weeks leads to severe congestion in the portal vein with infiltrate of inflammatory cells as well as fibroblastic cells proliferation which are extended in between the hepatocytes dividing the parenchyma into lobules. Also, brown pigments were detected in the portal area indicating a state of hepatocellular cholestasis. Undoubtly, our data fit with those recorded by Chen et al.<sup>[73]</sup> and Najmi et al.<sup>[74]</sup> These authors reported that the histopathological analysis of H and E-stained liver tissue sections of the TAA administered group reveals periportal necrosis and severe leucocytes infiltration.

The histological investigation of liver tissue sections of TAA administered group treated with BM-MSCs showed infiltration of inflammatory cells in the focal manner at the portal area and in diffuse manner between the hepatocytes. These findings are in accordance with those of Abdel Aziz et al.<sup>[61]</sup> and Hwang et al.<sup>[62]</sup> who observed that after MSC implantation, thickened septal fibrosis became thinner, collagen deposition decreased and periportal inflammation was alleviated.

## 5. CONCLUSION

Our results shed light on the therapeutic role of BM-MSCs in management of liver fibrosis in the experimental model. This was achieved *via* their capability to restore liver functions through their role in the extracellular matrix (ECM) organization and secretion of

antiapoptotic growth factor (HGF) which promoted regeneration of damaged liver tissue. Thus, this type of therapy represents a good remedy for treatment of human liver fibrosis.

## 6. ACKNOWLEDGMENT

The authors express their appreciation to Prof. Adel Bakeer Kholoussy, Professor of Pathology, Faculty of Veterinary Medicine, Cairo University for his kind cooperation in conducting histopathological investigation in the present study.

## 7. REFERENCES

- [1] Poynard T. Natural history of HCV infection. *Baillieres Best Pract Res Clin Gastroenterol*, 2000; 14: 211–28.
- [2] Davis GL, Albright JE, Cook SF, Rosenberg DM. Projecting future complications of chronic hepatitis C in the United States. *Liver Transpl*, 2003; 9:331–8.
- [3] Kuzu N, Metin K, Dagli AF, Akdemir F, Orhan C, Yalniz M, Ozercan IH, Sahin K. Protective Role of Genistein in Acute Liver Damage Induced by Carbon Tetrachloride. *Mediators inflamm*, 2007; 2007:36381.
- [4] Bataller R, Brenner DA. Hepatic stellate cells as a target for the treatment of liver fibrosis. *Semin Liver Dis*, 2001; 21:437–51.
- [5] Hammerman MR. Tissue engineering the kidney. *Kidney Int*, 2003; 63:1195-204.
- [6] Sipe JD. Tissue Engineering and Reparative Medicine. In: Sipe JD, Kelley CA, McNicol LA (eds.). *Reparative Medicine: Growing Tissues and Organs*, New York Academy of Sciences: 2002, pp.1-9.
- [7] Slack JM. Stem cells in epithelial tissues. *Science*, 2000; 287: 1431–3.
- [8] Alhadlaq A, Mao JJ. Mesenchymal stem cells: isolation and therapeutics. *Stem Cells Dev*, 2004; 13:436–48.
- [9] Rombouts WJ, Ploemacher RE. Primary murine MSC show highly efficient homing to the bone marrow but lose homing ability following culture. *Leukemia*, 2003; 17:160-70.
- [10] Peister A, Mellad JA, Larson BL, Hall BM, Gibson LF, Prockop DJ. Adult stem cells from bone marrow (MSCs) isolated from different strains of inbred mice vary in surface epitopes, rates of proliferation and differentiation potential. *Blood*, 2004; 103:1662-8.



- [11] Phinney DG, Kopen G, Isaacson RL, Prockop DJ. Plastic adherent stromal cells from the bone marrow of commonly used strains of inbred mice: variations in yield, growth and differentiation. *J Cell Biochem*, 1999; 72: 570-85.
- [12] Schäfer S, Calas A, Vergouts M, Hermans E. Immunomodulatory influence of bone marrow-derived mesenchymal stem cells on neuroinflammation in astrocyte cultures. *J Neuroimmunol*, 2012; 249: 40–8.
- [13] Wang HS, Hung SC, Peng ST, Huang CC, Wei HM, Guo YJ, Fu YS, Lai MC, Chen CC. Mesenchymal stem cells in the Wharton's jelly of the human umbilical cord. *Stem Cells*, 2004; 22:1330–7.
- [14] Qin H, Zhao L, Sun J, Ren L, Guo W, Liu H, Zhai S, Yang S. The differentiation of mesenchymal stem cells into inner ear hair cell-like cells *in vitro*. *ActaOto-Laryngologica*, 2011; 131: 1136-41.
- [15] Muñoz-Fernández R, Blanco FJ, Frecha C, Martín F, Kimatrai M, Abadía-Molina AC, García-Pacheco JM, Olivares EG. Follicular Dendritic Cells are Related to Bone Marrow Stromal Cell Progenitors and to Myofibroblasts. *J Immunol*, 2006; 177: 280-9.
- [16]. Lau HY, Bhatia M. Effect of CP-96,345 on the expression of adhesion molecules in acute pancreatitis in mice. *Am J Physiol Gastrointest Liver Physiol*, 2007; 292:1283–92.
- [17] Lee KD, Kuo TK, Whang-Peng J, Chung YF, Lin CT, Chou SH. *In vitro* hepatic differentiation of human mesenchymal stem cells. *Hepatology*, 2004; 40: 1275–84.
- [18] Horwitz EM, Prockop DJ, Fitzpatrick LA, Koo WW, Gordon PL, Neel M. Transplantability and therapeutic effects of bone marrow-derived mesenchymal cells in children with osteogenesis imperfecta. *Nat Med*, 1999; 5: 309–13.
- [19] Bergmeyer HU. Methods of enzymatic analysis. VerlagChemie, 1974; 2:735-9.
- [20] Mondzac A, Ehrlich GE, Seegmiller JE. An enzymatic determination of ammonia in biological fluids. *J Lab Clin Med*, 1965; 66:526.
- [21] Young DS, Pestaner LC, Gobberman V. Effects of drugs on clinical laboratory tests. *Clin Chem*, 1975; 21: 4310-20.
- [22] Handley DA, Hughes TE. Pharmacological approaches and strategies for therapeutic modulation of fibrinogen. *Thromb Res*, 1997; 87(1):1-36.
- [23] Wu C, Keivens VM, O'Toole TE, McDonald JA, Ginsberg MH. Integrin activation and cytoskeletal interaction are essential for the assembly of a fibronectin matrix. *Cell*, 1995; 83: 715–24.

- [24] Miyazawa K, Shimomura T, Naka D, Kitamura N. Proteolytic activation of hepatocyte growth factor in response to tissue injury. *J Biol Chem*, 1994; 269: 8966-8970.
- [25] Lowry OH, Rosebrough NJ, Farr AL, Randall RJ. Protein measurement with the folin phenol reagent. *J Biol*, 1951; 193:265-75.
- [26] Bancroft JD, Stevens A, Turner DR. Theory and practice of histological techniques. 4<sup>th</sup> Edit. In: Livingstone C and Philadelphia PA. (eds.). USA: 1996, pp. 25-90.
- [27] Armitage P, Berry G. Comparison of several groups. In: statistical method in medical research 2<sup>nd</sup> Ed. Blackwell significant publication, Oxford: 1987, pp.186-213.
- [28] Rochefort GY, Vaudin P, Bonnet N, Pages JC, Domenech J, Charbord P, Eder V. Influence of hypoxia on the domiciliation of mesenchymal stem cells after infusion into rats: possibilities of targeting pulmonary artery remodeling *via* cells therapies? *Respir Res*, 2005; 6:125.
- [29] Pittenger MF, Mackay AM, Beck SC, Jaiswal RK, Douglas R, Mosca JD, Moorman MA, Simonetti DW, Craig S, Marshak DR. Multilineage potential of adult mesenchymal stem cells. *Science*, 1999; 284:143-7.
- [30] Kumar BM, Maeng GH, Lee YM, Kim TH, Lee JH, Jeon BG, Ock SA, Yoo JG, Rho GJ. Neurogenic and cardiomyogenic differentiation of mesenchymal stem cells isolated from minipig bone marrow. *Res Vet Sci*, 2012; 93(2):749-57.
- [31] Li C, Kong Y, Wang H, Wang S, Yu H, Liu X, Yang L, Jiang X, Li L, Li L. Homing of bone marrow mesenchymal stem cells mediated by sphingosine 1-phosphate contributes to liver fibrosis. *J Hepatol*, 2009; 50:1174-1183.
- [32] Kawai K, Xue F, Takahara T, Kudo H, Yata Y, Zhang W, Sugiyama T. Matrix metalloproteinase-9 contributes to the mobilization of bone marrow cells in the injured liver. *Cell Transplant*, 2012; 21:453-464.
- [33] Wan M, Li C, Zhen G, Jiao K, He W, Jia X, Wang W, Shi V, Xing Q, Chen YF. Injury-Activated Transforming Growth Factor  $\beta$  Controls Mobilization of Mesenchymal Stem Cells for Tissue Remodeling. *Stem Cells*, 2012; 30:2498-511.
- [34] Wang J, Shin J, Choi M, Kim H, Son C. An herbal fruit, *Amomum xanthoides*, ameliorates thioacetamide-induced hepatic fibrosis in rat *via* antioxidative system. *J Ethnopharmacol*, 2011; 135:344-50.
- [35] Foo N, Lin S, Lee Y, Wu M, Wang Y.  $\alpha$ -Lipoic acid inhibits liver fibrosis through the attenuation of ROS-triggered signaling in hepatic stellate cells activated by PDGF and TGF- $\beta$ . *Toxicol*, 2011; 282:39-46.

- [36] Drotman RB, Lawhorn GT. Serum enzymes are indicators of chemical induced liver damage. *Drug and Chemical Toxicology*, 1978; 1: 163–71.
- [37] Ritzmann SE, Daniels JC. Little, Brown and Company, Boston. Serum Protein Abnormalities: Diagnostic and Clinical Aspects. *Ann Intern Med*, 1977; 86(4): 519.
- [38] Fontana L, Moreira E, Torres MI, Fernindez MI, Rios A, De Medina FS, Gil A. Serum amino acid changes in rats with thioacetamide-induced liver cirrhosis. *Toxicology*, 1996; 106:197-206.
- [39] Chang Y, Liu J, Lin P, Sun L, Peng C, Luo G, Chen T, Lee R, Lin S, Harn H, Chiou T. Mesenchymal stem cells facilitate recovery from chemically induced liver damage and decrease liver fibrosis. *Life Sciences*, 2009; 85:517–525.
- [40] Mehul D, Varsha G. Effect of polyherbal preparation on thioacetamide induced liver damage and hepatic encephalopathy in rats. *International research journal of pharmacy*, 2012; 3 (6): 192-8.
- [41] Nomura F, Ohnishi K, Terabayashi H, Nakai T, Isobe K, Takekoshi K, Okuda K. Effects of intrahepatic portal-systemic shunting on hepatic ammonia extraction in patients with cirrhosis. *Hepatology*, 1994; 20:1478–81.
- [42] Perez MJ, Suarez A, Gómez-Capilla JA, Sánchez-Medina F, Gil A. Dietary Nucleotide Supplementation Reduces Thioacetamide-Induced Liver Fibrosis in Rats. *J Nutr*, 2002; 132: 652–7.
- [43] Schuppan D. Structure of the extracellular matrix in normal and fibrotic liver. *Semin Liver Dis*, 1990; 10: 1–10.
- [44] Kossakowska A E, Edwards DR, Lee SS, Urbanski LS, Stabbler AL, Zhang CL, Phillips BW, Zhang Y, Urbanski SJ. Altered balance between matrix metalloproteinases and their inhibitors in experimental biliary fibrosis. *Am J Pathol*, 1998; 153: 1895–902.
- [45] Chijiwa K, Nakano K, Kameoka N, Nagai E, Tanaka M. Proliferating cell nuclear antigen, plasma fibronectin, and liver regeneration rate after seventy percent hepatectomy in normal and cirrhotic rats. *Surgery*, 1994; 116: 544–9.
- [46] Park JH, Kum YS, Lee TI, Kim SJ, Lee WR. Melittin attenuates liver injury in thioacetamide-treated mice through modulating inflammation and fibrogenesis. *Experimental Biology and Medicine*, 2011; 236: 1306–13.
- [47] Koenig W. Fibrinogen in cardiovascular disease: an update. *Thromb Haemost*, 2003; 89: 601–9.

- [48] Aster RH. Pooling of platelets in the spleen: role in the pathogenesis of "hypersplenic" thrombocytopenia. *J Clin Invest*, 1966; 45: 645.
- [49] Inagaki Y, Okazaki I. Emerging insights into transforming growth Factor  $\beta$ -Smad signal in hepatic fibrogenesis. *Gut*, 2007; 56: 284–92.
- [50] Liu X, Hu H, Yin JQ. Therapeutic strategies against TGF- $\beta$  signaling pathway in hepatic fibrosis. *Liver Int*, 2006; 26: 8–22.
- [51] Arteel GE. New role of plasminogen activator inhibitor-1 in alcohol induced liver injury. *J Gastroenterol Hepatol*, 2008; 23: S54–9.
- [52] Ignatz RA, Endo T, Massague J. Regulation of fibronectin and type I collagen mRNA levels by transforming growth factor- $\beta$ . *J Biol Chem*, 1987; 262: 6443–6.
- [53] Gressner AM, Weiskirchen R. Modern pathogenetic concepts of liver fibrosis suggest stellate cells and TGF- $\beta$  as major players and therapeutic targets. *J Cellular and Molecular Medicine*, 2006; 10: 76–99.
- [54] Shek FW, Benyon RC. How can transforming growth factor beta be targeted usefully to combat liver fibrosis? *European J Gastroenterology & Hepatology*, 2004; 16 (2): 123–126.
- [55] Bassiouny AR, Zaky AZ, Abdulmalek SA, Kandeel KM, Ismail A, Moftah M. Modulation of AP-endonuclease1 levels associated with hepatic cirrhosis in rat model treated with human umbilical cord blood mononuclear stem cells. *Int J Clin Exp Pathol*, 2011; 4(7):692.
- [56] Gressner AM, Weiskirchen R, Breitkopf K, Dooley S. Roles of TGF-beta in hepatic fibrosis. *Front Biosci*, 2002; 7(1): 793–807.
- [57] Schnur J, Oláh J, Szepesi A, Nagy P, Thorgeirsson SS. Thioacetamide induced hepatic fibrosis in transforming growth factor beta-1 transgenic mice. *Eur J Gastroenterol Hepatol*, 2004; 16:127–33.
- [58] Ling H, Roux E, Hempel D, Tao J, Smith M, Lonning S, Zuk A, Arbeeny C, Ledbetter S. Transforming Growth Factor  $\beta$  Neutralization Ameliorates Pre-Existing Hepatic Fibrosis and Reduces Cholangiocarcinoma in Thioacetamide-Treated Rats. *PLoS ONE*, 2013; 8(1):1–10.
- [59] Matsumoto K, Nakamura T. Hepatocyte growth factor: molecular structure, roles in liver regeneration, and other biological functions. *Crit Rev Oncogenesis*, 1992; 3: 27–54.

- [60] Naldini L, Vigna E, Narsimhan RP, Gaudino G, Zarnegar R, Michalo-poulos G K, Comoglio PM. Hepatocyte growth factor (HGF) stimulates the tyrosine kinase activity of the receptor encoded by the protoonco- gene *c-met*. *Oncogene*, 1991; 6: 501-4.
- [61] Abdel Aziz MT, Atta HM, Mahfouz S, Fouad HH, Roshdy NK, Ahmed HH, Rashed LA, Sabry D, Hassouna AA, Hasan NM. Therapeutic potential of bone marrow-derived mesenchymal stem cells on experimental liver fibrosis. *Clin Biochem*, 2007; 40: 893–9.
- [62] Hwang S, Hong HN, Kim HS, Park SR, Won YJ, Choi ST, Choi D, Lee SG. Hepatogenic differentiation of mesenchymal stem cells in a rat model of thioacetamide-induced liver cirrhosis. *Cell Biol Int*, 2012; 36: 279–88.
- [63] Puglisi MA, Tesori V, Lattanzi W, Piscaglia AC, Gasbarrini GB, D’Ugo DM, Gasbarrini M. Therapeutic Implications of Mesenchymal Stem Cells in Liver Injury. *Journal of Biomedicine and Biotechnology*, 2011; 1-8.
- [64] Sakaida I. Liver regeneration with the resolution of fibrosis by bone marrow cell infusion therapy. *New Frontiers in Regenerative Medicine*, 2007; 9-20.
- [65] Hinz B, Gabbiani G. Recent advances in myofibroblast biology and new therapeutic perspectives. *F1000. Biol. Rep*, 2010; 2: 78.
- [66] Ishikawa T, Banas A, Hagiwara K, Iwaguro H, Ochiya T. Stem cells for hepatic regeneration: The role of adipose tissue derived mesenchymal stem cells. *Curr Stem Cell Res Ther*, 2010; 5(2):182-9.
- [67] Saito Y, Shimada M, Utsunomiya T, Ikemoto T, Yamada S, Morine Y, Imura S, Mori H, Sugimoto K, Iwahashi S, Asanoma M. The protective effect of adipose-derived stem cells against liver injury by trophic molecules. *Journal of Surgical Research*, 2013; 180:162-8.
- [68] Crisostomo PR, Markel TA, Wang Y. Surgically relevant aspects of stem cell paracrine effects. *Surgery*, 2008; 143:577.
- [69] Cramer T, Schuppan D, Bauer M, Pfander D, Neuhaus P, Herbst H. Hepatocyte growth factor and c-Met expression in rat and human liver fibrosis. *Liver International*, 2004; 24(4): 335–44.
- [70] Maulik G, Shrikhande A, Kijima T, Ma PC, Morrison PT, Salgia R. Role of the hepatocyte growth factor receptor, c-Met, in oncogenesis and potential for therapeutic inhibition. *Cytokine Growth Factor Rev*, 2002; 13: 41-59.
- [71] Parekkadan B, van Poll D, Megeed Z, Kobayashi N, Tilles AW, Berthiaume F, Yarmush ML. Immunomodulation of activated hepatic stellate cells by mesenchymal

- stem cells. Biochemical and Biophysical Research Communications, 2007; 363:247–52.
- [72] Oyagi S, Hirose M, Kojima M, Okuyama M, Kawase M, Nakamura T, Ohgushi H, Yagi KJ. Therapeutic effect of transplanting HGF-treated bone marrow mesenchymal cells into CCl<sub>4</sub>-injured rats. Hepatol, 2006; 44:742–8.
- [73] Chen TM, Subeq YM, Lee RP, Chiou TW, Hsu BG. Single dose intravenous thioacetamide administration as a model of acute liver damage in rats. Int J Exp Path, 2008; 89: 223–31.
- [74] Najmi AK, Pillai KK, Pai SN, Akhtar M, Sharma M. Effect of l-ornithine l-aspartate against thioacetamide-induced hepatic damage in rats. Indian J of Pharmacology, 2011; 42:384-7.